O-5

ELSEVIER

Water Research 39 (2005) 3394–3408

WATER RESEARCH

www.elsevier.com/locate/watres

Modeling the dry-weather tidal cycling of fecal indicator bacteria in surface waters of an intertidal wetland

Brett F. Sanders[a,*], Feleke Arega[a,1], Martha Sutula[b]

[a]*Department of Civil and Environmental Engineering, University of California, Irvine, CA 92697-2175, USA*
[b]*Southern California Coastal Water Research Project, Westminster, California, USA*

Received 30 August 2004; received in revised form 19 May 2005; accepted 2 June 2005
Available online 26 July 2005

Abstract

Recreational water quality at beaches in California and elsewhere is often poor near the outlets of rivers, estuaries, and lagoons. This condition has prompted interest in the role of wetlands in modulating surface water concentrations of fecal indicator bacteria (FIB), the basis of water quality standards internationally. A model was developed and applied to predict the dry-weather tidal cycling of FIB in Talbert Marsh, an estuarine, intertidal wetland in Huntington Beach, California, in response to loads from urban runoff, bird feces, and resuspended sediments. The model predicts the advection, dispersion and die-off of total coliform, *Escherichia coli*, and enterococci using a depth-integrated formulation. We find that urban runoff and resuspension of contaminated wetland sediments are responsible for surface water concentrations of FIB in the wetland. Model predictions show that urban runoff controls surface water concentrations at inland sites and sediment resuspension controls surface water concentrations near the mouth. Direct wash-off of bird feces into the surface water is not a significant contributor, although bird feces can contribute to the sediment bacteria load. The key parameters needed to accurately predict FIB concentrations, using a validated hydrodynamic model, are: the load due to urban runoff, sediment erodibility parameters, and sediment concentrations and surface water die-off rates of enteric bacteria. In the present study, literature values for sediment erodibility and water column die-off rates are used and average concentrations of FIB are predicted within 1/2 log unit of measurements. Total coliform are predicted more accurately than *E. coli* or enterococci, both in terms of magnitude and tidal variability. Since wetland-dependent animals are natural sources of FIB, and FIB survive for long periods of time and may multiply in wetland sediments, these results highlight limitations of FIB as indicators of human fecal pollution in and near wetlands.

Keywords: Enteric bacteria; Intertidal wetland; Coastal; Water quality; Sediment

1. Introduction

Fecal indicator bacteria (FIB) groups such as total coliform (TC), fecal coliform (FC), *Escherichia coli* (EC), and enterococci (ENT) are utilized world wide to measure health hazards in bathing and shellfish harvesting waters (Thomann and Mueller, 1987). Water samples at popular beaches and harvesting waters are

*Corresponding author. Tel.: 949 824 4327; fax: 949 824 3672.
E-mail address: bsanders@uci.edu (B.F. Sanders).
[1]Presently, National Research Council Research Associate, US Environmental Protection Agency, Ecosystems Research Division, Athens, Georgia, USA.

0043-1354/$ - see front matter © 2005 Elsevier Ltd. All rights reserved.
doi:10.1016/j.watres.2005.06.004

routinely tested for FIB, which are thought to signal the presence of pathogens but are not necessarily pathogenic (US EPA, 1986). Chronic exceedances of California criteria have placed coastal water bodies such as Tomales Bay, Moss Landing Harbor, Morro Bay, Ventura Harbor, Marina Del Rey Harbor, Newport Bay, and Mission Bay on lists of pathogen impaired water bodies (CalEPA, 2002). Exceedances are also common at open ocean beaches, particularly near the outlets of storm drains, rivers, estuaries, and lagoons. Numerous coastal water bodies are impaired worldwide according to such standards.

Pathways by which FIB enter coastal waters include urban and agricultural runoff, waste water discharges, sewage leaks and spills, and fecal deposits by wildlife, notably birds. A complex web of processes influence the distribution of FIB in surface waters including flushing by ocean water, die-off, predation, sedimentation and resuspension, and regrowth on sediments, vegetation, and debris (Savage, 1905; Goyal et al., 1977; Roper and Marshall, 1979; Jensen et al., 1979; LaBelle et al., 1980; Grimes et al., 1986; Thomann and Mueller, 1987; Davies et al., 1995; Oshiro and Fujioka, 1995; Anderson et al., 1997; Byappanahalli and Fujioka, 1998; Solo-Gabriele et al., 2000; Grant et al., 2001). Use of FIB as indicators of human pathogens is complicated by these processes, particularly in wetlands where wildlife is abundant and nutrient rich sediments support growth of bacteria. So long as FIB remain the basis of regulations governing coastal water quality, a need will exist to identify the forcing factors (river inputs, storm drains, etc.) supporting FIB populations so that appropriate and cost-effective management measures can be implemented.

Several researchers have recently reported on models to predict FIB concentrations in coastal waters. Use of such models in coordination with field monitoring programs can help to identify the relative impact of various sources (e.g., a river versus a storm drain), characterize the mechanisms governing the fate of these organisms (e.g., flushing versus die-off) and predict the efficacy of a range of potential management measures. Kashefipour et al. (2002) used a model consisting of depth-integrated continuity, momentum, and transport equations to predict FIB concentrations in the Ribble Estuary, England. Fiandrino et al. (2003) used a model consisting of three dimensional continuity, momentum, and transport equations to predict FIB concentrations in Thau lagoon, France. Steets and Holden (2003) used a one-dimensional model to predict FIB concentrations in Arroyo Burro lagoon, California.

In this study we use a model to simulate dry-weather tidal cycling of TC, EC, and ENT concentrations in surface waters of Talbert Marsh, an intertidal wetland in Huntington Beach, California. Runoff from an urbanized watershed drains to the marsh, the marsh accommodates a high concentration of shore birds, and high sediment concentrations of FIB have been measured. Grant et al. (2001) reported that Talbert Marsh was a net source of ENT to coastal waters and hypothesized that it was due to a combination of bird feces and interactions with sediments and vegetation. Sediments act as a reservoir of FIB (Goyal et al., 1977, e.g.), and suspension and deposition cycles are germane to the estuarine environment (Mehta and Dyer, 1990). In Talbert Marsh, it is not clear whether FIB concentrations are predominantly controlled by urban runoff, erosion of contaminated sediments, bird feces, or some combination of these factors. Therefore, the model is applied to examine and rank the influence of these "forcing factors." The modeling effort described in this paper is unique relative to previously published studies in that non-point loads of FIB (bird feces, erosion of contaminated sediments) are incorporated into a multi-dimensional, time-dependent formulation for the first time.

The model in this study consists of depth-integrated continuity and momentum equations to simulate circulation, and depth-integrated transport equations to simulate surface water concentrations of FIB resulting from urban runoff, bird droppings and resuspended sediments. The model is parameterized using either in situ data or previously published values of model parameters. The model is applied to predict FIB over a 15 day period beginning May 2, 2000, coincident with an extensive field monitoring effort previously reported (Grant et al., 2001, 2002). This work demonstrates the power of first-principle models to elucidate the mechanisms and pathways by which near-shore coastal waters are polluted by FIB.

2. Methods and materials

2.1. Site description

Talbert Watershed, shown in Fig. 1, is a 3300 ha catchment along the southern California coastline in the cities of Huntington Beach and Fountain Valley. On average, the watershed receives 29 cm of rainfall, over 90% of which falls between November and April. Daily high/low temperatures average 23/17 °C in September and 17/8 °C in January. The watershed slopes mildly (10^{-4}) towards the ocean and is drained by a network of channels that, due to the low elevation and mild slope of the watershed, are flooded by tides. Talbert Channel is the main stem of the network. Inland 2 km from the mouth, Huntington Beach Channel branches west and extends 5 km inland; and 8 km from the mouth, Fountain Valley Channel branches east. High tide floods Talbert Channel to the Fountain Valley Channel junction and the length of the Huntington Beach channel. Depths in the channels are comparable to the

Fig. 1. View of Talbert Marsh, channel network, and surrounding watershed as low tide. Channels and watershed extends several kilometers further inland than indicated in the figure. At high tide, the southwestern and southern portions of Talbert Marsh are flooded. PCH, BRK, and AES indicate monitoring stations.

tidal amplitude, roughly 1 m. Near the outlet, Talbert Marsh occupies roughly 10 ha of what used to be an extensive (1200 ha) tidal marsh environment that was filled for development over the past century. Talbert Marsh was created in 1990 when remnant marsh was flooded following the removal of a Talbert Channel levee. The channel bed consists of beach sand and silts near the outlet and within a flood delta that penetrates a short distance into the marsh. Further inland, the marsh and channel bed consists of organic rich silts and muds, except the upper reaches of Talbert Channel and Fountain Valley Channel where the bed is lined with concrete. In this study, the Talbert Marsh and tidal channels are collectively referred to as the wetland. From a perspective of flushing the wetland may be divided into two zones: a poorly mixed zone inland where residence times are at least a week, and a well-mixed zone near the mouth that is flushed each tide cycle with ocean water. The interface between these zones oscillates with the ebb and flow of the tides.

The watershed is heavily developed as is common to the greater Los Angeles basin, and it contains separate networks of storm and sanitary sewers. Storm sewers direct runoff into street drains that funnel to the wetland. In the lower half of the watershed where the topography is lowest, runoff collects in one of several roughly 500 m^3 forebays that are intermittently drained by pump stations. A program is now in place to divert dry-weather runoff from the storm sewer to the sanitary sewer for treatment. This program began on a limited basis in Fall 1999 and encompassed the entire watershed by Summer 2001. During the 15 day period that is the focus of this study, pump stations were operated in two different modes. During the first 8 days, pumpstations were not activated so runoff either collected in the forebay or was diverted to the sanitary sewer system.

During the remaining 7 days, pumpstations intermittently discharged untreated runoff to the channel network. Over the entire 15 day period, there was dry-weather baseflow in Talbert Channel that entered the wetland.

Monitoring stations referenced in this paper include Pacific Coast Highway (PCH), Brookhurst Street (BRK), and AES Corp. (AES). These are shown in Fig. 1.

2.2. FIB modeling

A hydrodynamic model was developed to simulate surface water concentrations of FIB in the wetland, from the outlet of Talbert Marsh to the head of the Huntington Beach Channel and, along Talbert Channel, to the Fountain Valley Channel junction. The model consists of depth-integrated continuity, momentum, and transport equations (Arega and Sanders, 2004), similar to the approach adopted by Kashefipour et al. (2002). The flow equations (continuity and momentum) were forced by the ocean tide just offshore of the marsh, and by runoff flowing into the upper reaches of the wetland. Ocean tide forcing was based on tide levels recorded at NOAA station 9410660, Los Angeles and archived online at `http://tidesonline.nos.noaa.gov/`. The discharge of runoff at the Talbert Channel inflow boundary, Q_R, was assumed steady over the study period. To model pumpstation operations, the discharge of runoff from each pumpstation, Q_P, was assumed uniform and steady over the final seven days of the study period, but zero over the first eight days. Seven pumpstations that discharge directly into the wetland were incorporated into the model. Runoff data (Q_R and Q_P) were obtained from other reports (Grant et al., 2001, 2002; Chu, 2001) and appear in Table 1. Topographic data necessary for flow predictions were obtained from as-built plans of the concrete-line portions of the channels and a field survey of the Talbert Marsh (Chu, 2001). A uniform Manning coefficient was used to account for bed resistance (Arega and Sanders, 2004).

Simultaneous with the flow prediction described above, surface water FIB were predicted by solving the following transport equations:

$$\frac{\partial}{\partial t}(hc_i)+\frac{\partial}{\partial x}(\bar{u}hc_i)+\frac{\partial}{\partial y}(\bar{v}hc_i) = \frac{\partial}{\partial x}\left(hE_{xx}\frac{\partial c_i}{\partial x}+hE_{xy}\frac{\partial c_i}{\partial y}\right) + \frac{\partial}{\partial y}\left(hE_{yx}\frac{\partial c_i}{\partial x}+hE_{yy}\frac{\partial c_i}{\partial y}\right) - hl_i+a_i+\sum_{k=1}^{N_{PS}}\mathscr{L}_{ik}\,\delta(x-x_s^k,y-y_s^k), \quad (1)$$

where h = depth [m] and $\bar{u}$, $\bar{v}$ = components of the depth-averaged fluid velocity [m/s], E_{xx}, E_{xy}, E_{yx}, and E_{yy} = elements of the dispersion tensor [m^2/s], c_i, $(i=1,\ldots,N_b)$ = water column concentration of FIB [MPN/m^3], N_b = number of FIB groups tracked by the model, l_i = water column loss rate [MPN/m^3/s], a_i = flux of FIB to water column at sediment/water interface [MPN/m^2/s], and $\mathscr{L}_{ik}$ = FIB loading rate of the ith FIB group at the kth inflow point [MPN/s], N_{PS} is the

Table 1
Measured, cited, and computed parameters used to estimate loading and die-off models

Parameter	Units	Total coliform		*E. coli*		Enterococci	
		Value	Uncertainty	Value	Uncertainty	Value	Uncertainty
k[a]	m^2/Watts/h	0.0018	±10%	0.0017	±10%	0.00097	±10%
c_R[b]	MPN/100 mL	1.5×10^4	$2.2\times10^4/1.0\times10^4$	9.8×10^2	$1.4\times10^3/7.1\times10^2$	1.8×10^3	$2.4\times10^3/1.3\times10^3$
r[b]	MPN/bird/day	2.8×10^7	$8.4\times10^7/2.1\times10^6$	1.5×10^7	$1.0\times10^8/1.2\times10^7$	7.2×10^6	$2.6\times10^7/5.2\times10^6$
s[b]	MPN/g	5.2×10^3	$1.3\times10^4/2.0\times10^3$	2.1×10^2	$8.5\times10^2/5.1\times10^1$	6.8×10^2	$1.6\times10^3/2.9\times10^2$
Parameter	Units	Value	Uncertainty (%)	Parameter	Units	Value	Uncertainty (%)
Q_R	m^3/d	1000	±50	$\overline{n_b}$	—	174	±50
Q_P	m^3/d	300	±50	$\langle\bar{\tau}\rangle$	Pa	0.08	±50
$\overline{A_S}$	ha	32	±50	τ_0	Pa	0.75	±50
E_0[c]	kg/m^2/s	1×10^{-4}	±50	τ_c[c]	Pa	0.25	±50

Except where noted, a conservative estimate of 50% uncertainty was adopted. Note that the mathematical model is presented using SI units, so conversion factors need not appear in model equations. Commonly used units are presented here to facilitate comparison with previous works and other studies.

[a]Die-off rates based on Sinton et al. (1999).

[b]Measured in situ, uncertainty based on standard error.

[c]Erodibility rates based on Uncles and Stephens (1989).

number of inflow points where runoff is added to the wetland (pump stations and tributary inflow), x_s^k and y_s^k = coordinates of each inflow point [m], and δ = Dirac delta function [1/m^2]. The dispersion tensor accounts for longitudinal dispersion (Elder, 1959) and transverse mixing (Ward, 1974), and it is computed locally depending on the orientation of the currents (Arega and Sanders, 2004). Note that SI units are adopted for the purpose of presenting the mathematical model, so conversion factors need not appear in model equations. However, many model parameters are reported in Table 1 with commonly used units to facilitate comparison with previous works and other studies.

Eq. (1) was solved using $N_b = 9$ to predict the distribution of TC, EC, and ENT resulting from urban runoff, bird feces, and sediment resuspension. Groups 1–3 correspond to TC, EC, and ENT concentrations resulting from runoff sources, 4–6 from bird sources, and 7–9 from sediment sources. All model predictions account for surface water die-off using first order kinetics as follows:

$$l_i(x, y, t) = k_i I(t) c_i(x, y, t), \tag{2}$$

where k_i = die-off rate constant [m^2/Watts/s] based on Sinton et al. (1999), and $I(t)$ = solar intensity [Watts/m^2]. Die-off rates used in the model were taken from Sinton et al. (1999), and solar intensity data for the study period were obtained from Grant et al. (2001).

The model does not account for settling. Suspended sediments in the 1–10^3 μm size range are typical of intertidal wetlands adjacent to sandy ocean beaches, but FIB in southern California coastal waters are either free-living (planktonic, roughly 1 μm in size) or associated with very fine sediments, probably in the 10 μm range or less (Ahn et al., 2005). The relative influence of settling and die-off is defined by the ratio $w_s/k_i Ih$, where w_s is the settling velocity. Using Stokes Law to model the settling velocity in terms of particle size (e.g. Nazaroff and Alvarez-Cohen, 2001, Chapter 4), the average solar radiation rate for the study period (288 Watts/m^2), die-off rates reported by Sinton et al. (1999), and a depth of 1 m which is typical for the wetland, this ratio is unity for ENT when particle diameter $d = 10$ μm and for TC and EC when $d = 13$ μm. When $d = 5$ μm, this ratio is 0.3 for ENT and 0.2 for TC and EC. The nonlinear dependence is due to the quadratic relationship between settling velocity and particle size. Without a clear understanding of the partitioning of FIB between free-living and particle-associated states, and knowledge of the median diameter of particles with attached FIB, selecting an appropriate settling velocity is difficult. Certainly, without settling terms the model will underestimate water column FIB losses if these organisms are associated with particles in the 10–20 μm range or larger. Therefore, this assumption should be reconsidered if the model significantly overpredicts FIB concentrations.

For all predictions, the concentration of FIB in water entering the wetland from the ocean was set to zero. For the urban runoff predictions ($i = 1$–3), point loads of FIB were specified at runoff inflow points and the non-point loading term, a_i, was set to zero. The loading rate was set equal to the volumetric flow rate multiplied by the concentration of FIB in runoff, c_R, which was specified based on average Talbert Watershed urban runoff concentrations reported by Reeves et al. (2004).

FIB loading to surface waters by bird feces ($i = 4$–6) was modeled as a spatially distributed (around the water line) and temporally variable non-point source. It was assumed that all bird feces fell exclusively on the shoals of the marsh, were subject to sunlight induced die-off, and upon flooding by the tide were instantaneously and completely transferred to the water column. Hence, loading in the model occurs at water's edge during the rising tide. This approach was motivated by bird surveillance data, which showed birds congregated on shoals during low tides (Grant et al., 2001). The following mass balance equation was solved to track the build-up an die-off of FIB on the shoals of the marsh,

$$\frac{dm_i(x, y, t)}{dt} = d_i(t) - k_i I(t) m_i(x, y, t), \tag{3}$$

where m_i = the surficial FIB density [MPN/m^2] and d_i = FIB loading rate [MPN/m^2/s]. Note that the die-off rate constant for the marsh banks is identical to that used for surface water. The FIB loading rate was computed as,

$$d_i(t) = n_b(t) r_i / A_{IT}(t), \tag{4}$$

where $A_{IT}(t)$ = the exposed (or dry) inter-tidal surface area [m^2], $n_b(t)$ = bird population measured hourly in the marsh and r_i = rate of FIB loading per bird [MPN/bird/s]. The exposed inter-tidal surface area (or area of the exposed shoals) was determined from the marsh topography as the difference between the exposed surface area of the marsh and the exposed surface area under high spring tide conditions. This varied from 0 to 4.5 ha depending upon the tide stage. Table 1 presents bird loading rates used in the model, which were based upon samples collected Talbert Marsh. The sampling methodology is described in (Grant et al., 2001), but only ENT concentrations are reported. TC and EC were quantified from the same samples using defined substrate tests (IDEXX, Westbrook, Maine), but the data have not previously been reported.

FIB loading rates of birds vary widely depending upon species, habitat, diet, and feeding habits. Hussong et al. (1979) reported fecal coliform loading rates for wild swan and Canadian geese of 10^6–10^9 and 10^4–10^7 MPN/bird/day, respectively, Gould and Fletcher (1978)

reported fecal coliform loading rates for several gull species in the range of 10^6–10^7 MPN/bird/day. Alderisio and DeLuca (1999) reported fecal coliform loading rates of roughly 10^8 and 10^5 MPN/bird/day for ring-billed gulls and Canadian geese, respectively. Rates reported in Table 1 for shore birds in Talbert Marsh are similar, roughly 10^7 MPN/bird/day for all three indicator groups. During the study period bird populations ranged from 0 to 1180 (Grant et al., 2001).

After being flooded by the rising tide, the wash-off of surficial bacteria from the marsh banks contributes to the sediment/water interface loading rate, a_i appearing in Eq. (1), as follows:

$$a_i(x, y, t) = m_i(x, y, t)\delta(t - t_f), \tag{5}$$

where t_f = the instant land is flooded by the rising tide [s] and δ = Dirac delta function [1/s]. Hence, the transfer of surficial FIB from the banks of the marsh to surface waters is modeled as an instantaneous exchange that is triggered by moment the bank is flooded by the rise of the tide. After transfer to surface waters, $m_i = 0$ until the banks are again dry at which point the build-up process resumes.

FIB loading to surface waters by sediments ($i = 7$–9) was modeled as a spatially distributed and temporally variable non-point. The non-point loading term a_i in Eq. (1) was formulated to account for the transfer of FIB to the water column that occurs when FIB laden particulate matter and pore water on the bed is mobilized by turbulent shear. The mobilization of estuarine sediments occurs after a threshold in turbulent shear has been exceeded, and in proportion to the excess of turbulent shear above the threshold (Partheniades, 1965; Mehta and Dyer, 1990). Whether or not the same is true for FIB is not clear, for FIB may be free living in sediment pore water, attached to sediment grains, or incorporated into microbial biofilms; and how these phases of FIB respond to shear is not known. Therefore, a novel approach was taken. The FIB loading term was developed by dimensional analysis with the following conditions in mind: (a) that the transfer rate of FIB from sediments to surface waters be proportional to the shear rate; and (b) that FIB liberated from the sediments over a tide cycle be equal to FIB present (either attached to particles or free-living in pore water) in the erodible layer of surficial sediments. Therefore, the following rate expression was used,

$$a_i(x, y, t) = s_i E \frac{\tau(x, y, t)}{\tau_0}\left(\frac{\tau_0}{\tau_e} - 1\right), \tag{6}$$

where s_i = geometric mean concentration of FIB per mass of sediment [MPN/kg], E = entrainment rate parameter [kg/m^2/s], τ = spatially and temporally varying shear stress at the bed [Pa] computed by the hydrodynamic model, τ_e = critical shear stress for erosion [Pa], and τ_0 = reference stress [Pa] representative of erosive conditions in the wetland.

The reference stress was computed based on water level and velocity data collected at BRK (Arega and Sanders, 2004). BRK serves as a good reference point due to its central location. Using a drag coefficient of 0.003 which is typical of estuaries, a fluid density of 1 g/cm^3, and a velocity of 0.5 m/s, the reference stress was estimated to be $\tau_0 = 0.75$ Pa. A velocity of 0.5 m/s was used for this calculation since the peak flood velocity varies from 0.4 to 0.6 m/s over the spring-neap cycle, while the peak ebb velocity varies from 0.1 to 0.4 m/s. Site specific entrainment rate and critical shear parameter estimates were not available, so values reported in the literature by Uncles and Stephens (1989) and Tattersall et al. (2003) were used. All model parameters are reported in Table 1.

Note that measured concentrations of FIB in Talbert Marsh sediments were utilized to estimate s_i. No attempt was made to model the cycling of FIB in submerged sediments. To estimate the concentration of FIB in sediments, cores were collected at low tide within the inter-tidal zone and immediately transported to the laboratory. Overlying water was siphoned off the top and the cores were sectioned in 1 cm intervals with an extruder. For the few cores with a high sand content, sediment was scraped from the core tube in specified intervals to avoid slumping. Each sediment section was homogenized. A 5 g sample was suspended with 45 ml of a 0.5 M mono potasium phosphate buffer solution in a sterilized glass centrifuge tube for enteric bacteria analysis (APHA, 1992, Methods 9221 and 9050C). The sample was agitated for 1 min with a vortex mixer, then centrifuged at 2000 rpm for 5 min. The supernatant was then analyzed for TC, EC, and ENT using defined substrate tests with dilutions to the supernatant made with DI water (IDEXX, Westbrook, Maine). The remaining sediment from each 1 cm section was oven dried at 50 °C, and stored for analysis of grain size. The concentration s_i was taken as the geometric mean of FIB concentrations in the top 1 cm of each sample, and is reported in Table 1.

An important assumption of this formulation is that sediment concentrations are constant over the two-week study period. Unpublished sediment data collected on a daily to weekly basis in nearby Santa Ana River wetlands show sediment concentrations of FIB increase at least one log unit immediately following storms, and subsequently decrease over a period of several days to weeks; but during dry-weather periods sediment concentrations are relatively uniform (Ambrose, 2004). This assumption would no longer be appropriate were the model used for wet-weather conditions or to predict variability on seasonal time scales.

The hydrodynamic equations, FIB transport equations, and mass balance equation for FIB build-up/

die-off on inter-tidal mudflats were integrating using a common time step of 0.2 s on an unstructured grid of 11732 quadrilateral cells encompassing all the wetted and inter-tidal portions of the channel network shown in Fig. 1. The flow and transport equations were solved by a finite volume numerical method described and validated for this study site by Arega and Sanders (2004). The build-up/die-off model for the load due to bird feces was solved using a backwards Euler discretization, for stability purposes and without concern for time-stepping errors due to the very small time step. The time of flooding, t_f appearing in Eq. (5) is determined in the model as the moment that all four nodes of a cell first become submerged by the rising tide. The solution of this model gives a spatially and temporally varying prediction of FIB concentrations in the wetland resulting from loading by urban runoff, bird feces, and sediment resuspension.

To summarize, nine different FIB concentration fields were predicted for the 15 day period beginning May 2, 2000 based on three different sources of three different FIB groups. Urban runoff loads were modeled by several point sources located at inland sites. Bird feces loads were modeled by a build-up, wash-off model: bacteria concentrations build up on inter-tidal mudflats and wash off (to surface waters) with the rising tide. Sediment loads were modeled by a non-point source that is scaled by the shear stress on the bed. For all nine predictions, the model accounts for FIB advection, dispersion, and die-off. Initial conditions for the model were obtained by a spin-up procedure. Starting with an FIB concentration of zero, predictions were made for two sequential 15 day periods, and results of the second 15 day period were saved and used for analysis purposes. Forcing data such as the ocean tide record, solar radiation data, and bird census data were simply duplicated into 30 day records. Finally, predictions were compared to FIB measurements at PCH and BRK monitoring stations (Fig. 1) reported by Grant et al. (2001, 2002). Water level, velocity, and turbidity data for PCH and BRK reported by Grant et al. (2001) were also utilized for model validation purposes.

2.3. Uncertainty in Model Predictions

Uncertainty in FIB predictions is due to several factors including: (a) approximations inherent to the mathematical representation of FIB transport processes; (b) errors incurred during the numerical solution of the mathematical model; and (c) uncertainty in model parameters and in particular, parameters that characterize point and non-point loads of FIB. Uncertainties in parameter values were estimated based on standard errors or literature reported values, where possible. Otherwise, a conservative estimate of 50% was used. Table 1 presents uncertainty estimates. In cases involving FIB concentrations, uncertainties may be 200–500%. By comparison, uncertainty associated with the mathematical model and numerical method are relatively small, roughly 20% and 1%, respectively, based on previous modeling efforts (Arega and Sanders, 2004). Therefore, the propagation of uncertainty in the model was ignored for the purpose of determining uncertainties in predicted FIB concentrations, and emphasis was placed on the uncertainty in loading terms (Holman, 1978). Hence, the relatively uncertainty in FIB predictions was assumed to be equal to the relative uncertainty in the corresponding FIB load. Based on the preceding model formulation for urban runoff, bird, and sediment loads of FIB, spatially and temporally averaged loading rates follow as:

$$L_R = (Q_R + 7Q_P)c_R, \tag{7}$$

$$L_B = \overline{n_b} r, \tag{8}$$

$$L_S = sE\frac{\langle\overline{\tau}\rangle}{\tau_0}\left(\frac{\tau_0}{\tau_c} - 1\right)\overline{A_S}, \tag{9}$$

where the overbar notation indicates a time-average value, the angled brackets indicate a spatial average, A_S represents the submerged surface area of the wetland, and the subscripts R, B, and S denote loads from runoff, bird droppings, and sediments, respectively. The upper limit of uncertainty was estimated by a conventional variational method (Taylor and Kuyatt, 1994), but this method predicted negative loads at the lower limit. Hence, the lower limit of the loads were estimated by computing the load based on lower limit parameter values. After upper and lower uncertainties for each of the nine FIB loads were estimated, these were normalized by the corresponding load to obtain relative uncertainties.

3. Results

Model predictions of water level and velocity during the study period compare well to measurements, as shown in Fig. 2. This indicates that the dominant circulation pattern in the wetland, which drives the mixing and flushing of FIB, is resolved. The spatial distribution of TC predictions at mid-flood tide are shown in Fig. 3 for the case of loading by bird feces (left panel), urban runoff (center panel) and sediment resuspension (right panel). For the case of loading by urban runoff, where FIB enter the wetland far inland along the channels and transport to the marsh during the ebb, the mid-flood condition highlights the transport of (assumed to be) FIB-free ocean water into the main channel of the marsh while remnant wetland water is displaced either into the fringes of the marsh or inland along the channels (note the gradient in FIB between the

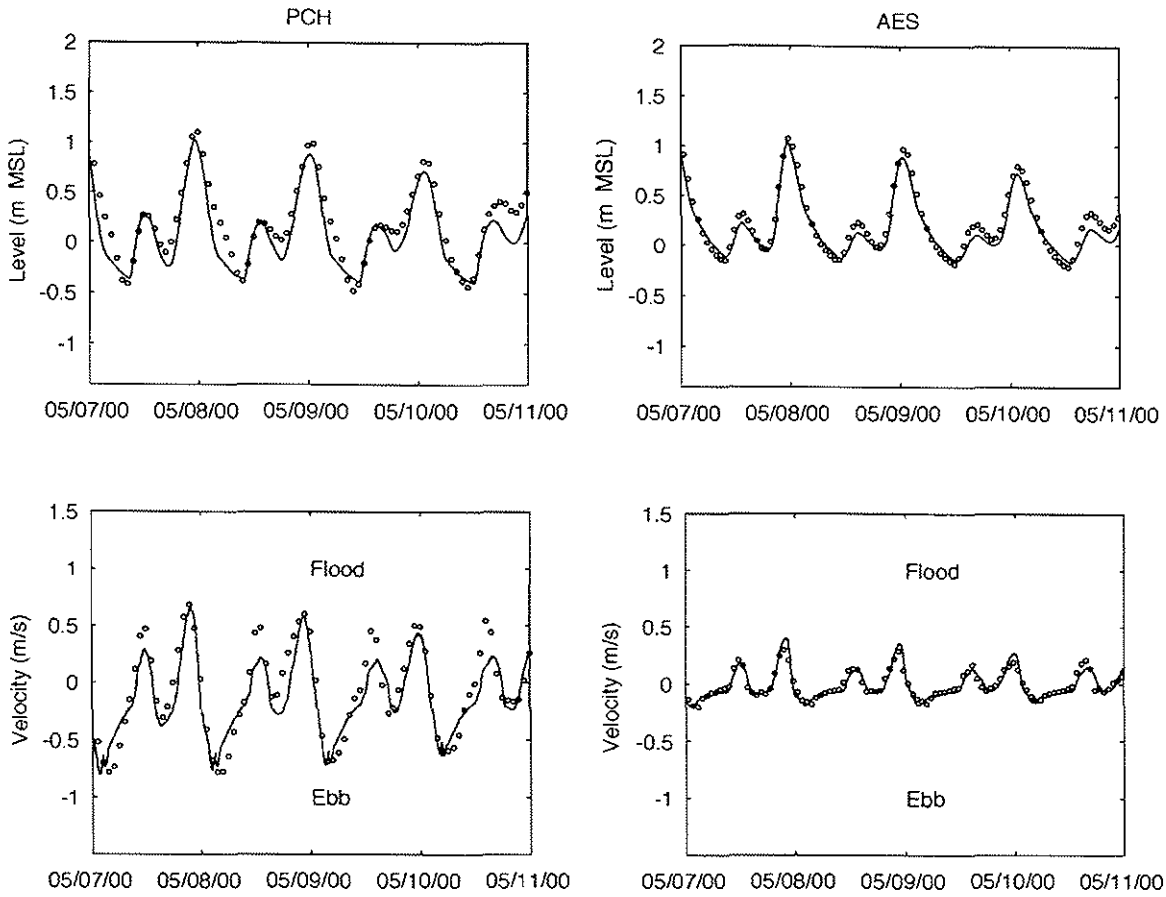

Fig. 2. Comparison of model predicted water level (top) and velocity (bottom) to data reported by Grant et al. (2001). Solid line corresponds to model prediction, symbols correspond to data.

main channel and the fringes of the marsh). For the case of loading by bird feces, model predictions illustrate the concentration of TC near the banks and over the shoals of the marsh. This is an expected response since FIB loading is modeled at the interface between wet and dry land. For the case of loading by sediment resuspension, FIB concentrations are relatively uniform across the marsh, compared to forcing by urban runoff or bird droppings. A similar distribution is predicted for EC and ENT.

Model predictions and measurements of FIB for the two-week study period are shown for BRK and PCH in Figs. 4 and 5, respectively, along with water level and turbidity. The tide record shows the spring-neap-spring transition. Note that water levels in the marsh do not drop far below −0.5 m–MSL due to hydraulic choking which occurs during the ebb at the outlet, where the minimum bed elevation is close to −0.7 m–MSL. FIB predictions vary considerably depending upon the type of loading, both in terms of magnitude and variability, particularly at 1 and 2 cycles per day. In addition, the variability of each prediction appears unique. Therefore, the phasing and magnitude of FIB predictions for each load type (i.e., urban runoff, bird feces, or sediment) can be utilized to help determine the contribution towards observed FIB concentrations. Pearson correlation coefficients were computed to quantify how well each prediction captured the variability, or phasing, of measured FIB concentrations and are shown in Table 2. Mean values of each prediction, and uncertainty based on loading rate uncertainty, are listed in Table 3. Mean values of measured FIB, along with standard errors based on $N = 360$ are also shown for comparison purposes. The "combined" FIB time series referenced in Tables 2 and 3 represent the sum of the three FIB predictions (i.e., urban runoff, bird feces, and sediment), a valid operation for linear transport equations. That is, the combined FIB time series is precisely what the model would have predicted had each of the forcing factors been incorporated into a single

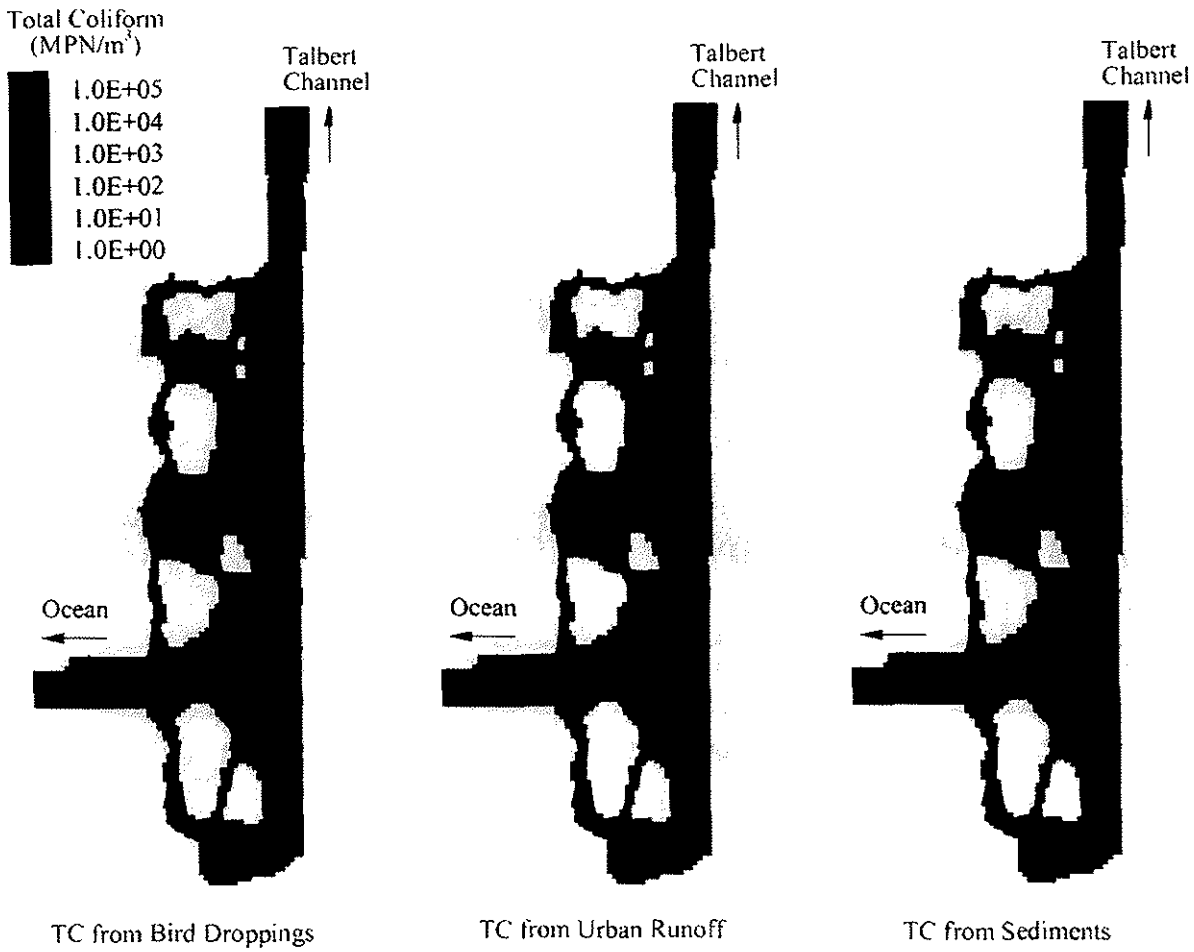

Fig. 3. Contours of total coliform in Talbert Marsh predicted by the model for mid-flood tide. Black lines indicate velocity direction and relative magnitude.

simulation. To obtain the mean value, the combined time series was first log-transformed. The combined series is not shown in Figs. 4 and 5, but at any given instant it basically tracks the largest of the three curves representing different forcing factors.

TC at PCH are predicted remarkably well based on loading by sediment resuspension, as shown in Fig. 5. The mean of log transformed measurements, log 10(TC) $= 2.17(\pm 0.04)$, or "log mean", compares well with the log mean of predictions log 10(TC) $= 2.25(+0.45/-1.02)$; and there is a moderate correlation ($R^2 = 0.58$, $p_{N=360} < 0.01$) between log transformed predictions and measurements on an hourly basis. Predictions based on loading by urban runoff compare best to measurements at the end of the ebb tide, particularly during the second week of the study when pump stations contributed runoff to the channels, but not at other phases of the tide and this is reflected by a weaker but significant correlation ($R^2 = 0.37$, $p_{N=360} < 0.01$). Predictions based on bird feces loading appear at least three orders of magnitude too small to account for observed TC.

Similar trends can be observed at BRK. Predictions based on both urban runoff and sediment loading are large enough to account for measured FIB, though in this case measurements correlate better to the prediction based on runoff ($R^2 = 0.56$, $p_{N=360} < 0.01$) than sediment resuspension ($R^2 = 0.26$, $p_{N=360} < 0.01$). The prediction based on bird feces loading is too small to account for observed TC. When predictions based on all three forcing factors are added together (valid for linear tranport equations), the prediction at BRK correlates slightly better ($R^2 = 0.58$, $p_{N=360} < 0.01$) and the magnitude of the signals compare well (Table 3).

For ENT and EC, trends in model predictions are similar to TC. However, trends in measured FIB differ. Both ENT and EC measurements compare best to predictions based on sediment resuspension loading, both in terms of geometric mean concentrations

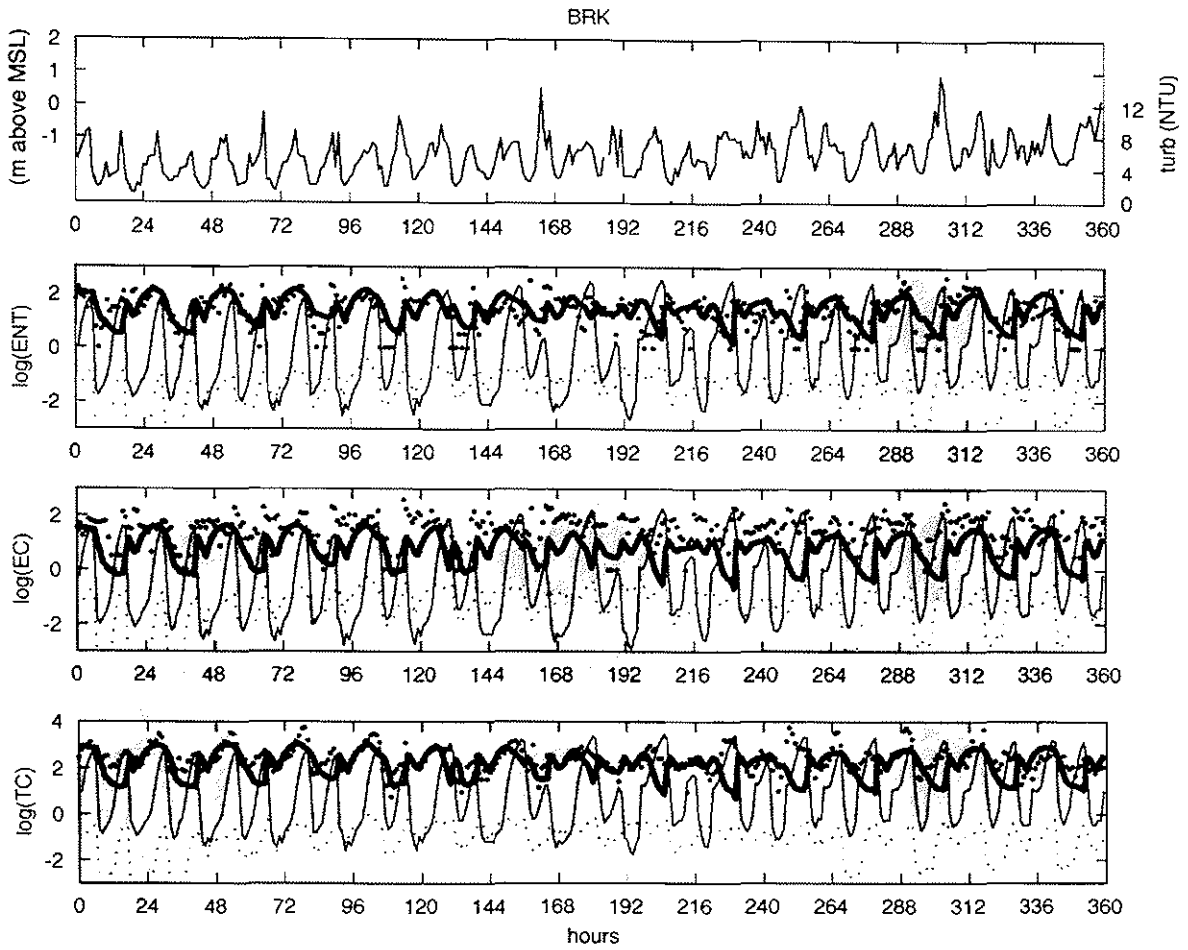

Fig. 4. BRK results. Water level and turbidy reported by Grant et al. (2001) shown in top panel. Bottom three panels show FIB concentrations: data from Grant et al. (2001, 2002) (dots), prediction based on sediment loading (heavy line), prediction based on runoff loading (light line), and prediction based on bird loading (broken line). FIB concentrations reported as log 10 (MPN/100 ml).

(Table 3) and the correlation coefficient (Table 2). Predictions based on bird feces loading are several log units too small to account for measured concentrations. Predictions based on urban runoff loading are comparable in magnitude only at the end of the ebb tide, and do not correlate to measurements.

Correlations between turbidity measurements and FIB measurements over the first six days were also computed and these appear in Table 4 (Due to drift in the turbidity data, the second week of data was excluded.) Turbidity correlates best to TC, compared to ENT and EC, and the correlation is stronger at BRK than PCH. Correlations between turbidity measurements and FIB predictions based on loading by urban runoff and sediment resuspension were also computed. Predictions based on urban runoff loads serve as an index of particulate material transported from upstream (fine mineral particles, detritus, and plankton) where flow is quiescent, while predictions based on sediment loads serve as an index of material eroded locally in the lower reaches of the wetland where the shear is greatest. At BRK the turbidity signal correlates better with FIB predictions based on runoff forcing ($R^2 = 0.70$, $p_{N=144} < 0.01$) than FIB predictions based on sediment resuspension forcing ($R^2 = 0.19$, $p_{N=144} < 0.01$). At PCH the turbidity signal correlates slightly better with the prediction based on sediment resuspension ($R^2 = 0.57$, $p_{N=144} < 0.01$) than the prediction based on runoff ($R^2 = 0.47$, $p_{N=144} < 0.01$).

4. Discussion

Hydrodynamic model predictions show that tidal cycling of TC, EC, and ENT in Talbert marsh surface waters is driven primarily by two processes: advection of

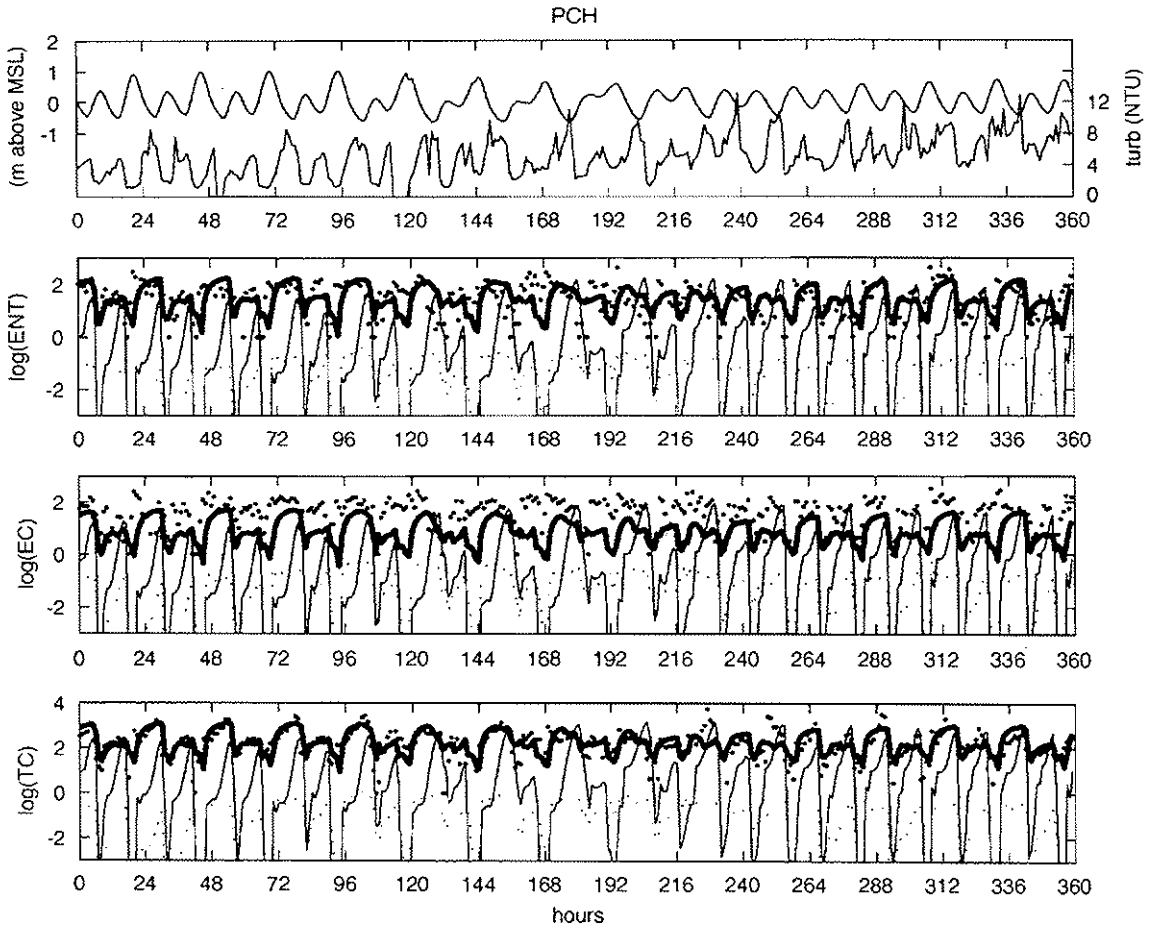

Fig. 5. PCH results. Water level and turbidy reported by Grant et al. (2001) shown in top panel. Bottom three panels show FIB concentrations: data from Grant et al. (2001, 2002) (dots), prediction based on sediment loading (heavy line), prediction based on runoff loading (light line), and prediction based on the bird loading (broken line). FIB concentrations reported as log 10 (MPN/100 ml).

FIB from inland sources (urban runoff) and entrainment of FIB from sediments. Loads of FIB from urban runoff control surface water concentrations inland within the poorly flushed zone while tidal resuspension controls surface water concentrations in the well-flushed zone near the mouth. Therefore, water quality models for FIB in hydrodynamically active wetland surface waters should at minimum account for loads from point sources (storm drains, channels, etc.), loads from resuspended sediments, transport by advection and turbulent dispersion/diffusion, and die-off. The present model captures tidal variability of TC better than EC or ENT suggesting either that processes important to EC and ENT transport are not included in the model, or perhaps the model oversimplifies one or more of the processes that are included in the model. For example, the spatial distribution of EC and ENT in sediments may differ substantially from the TC distribution due to differences in survival and/or regrowth rates. Many studies have shown that FIB can survive for long periods or regrow attached to sediments and vegetation (Savage, 1905; Roper and Marshall, 1979; LaBelle et al., 1980; Davies et al., 1995; Desmarais et al., 2002). In tropical watersheds, regrowth has been cited as the dominant factor affecting bacteria loading in streams (Hardina and Fujioka, 1991; Fujioka et al., 1999). The ability of bacteria to secrete extracellular polymers (collectively termed microbial biofilms) may be one reason why survival and regrowth of FIB is enhanced in sediments (Decho, 2000). A model capable of simulating sediment concentrations of FIB, accounting for these factors, might lead to better EC and ENT predictions. In cases where the size of particles with attached FIB is known, settling can also be included in the model if size

Table 2
Pearson correlation between log transformed enteric bacteria measurements and model predictions ($N = 360$)

	Station	Bird source	Sed. source	Runoff source	Combined
Total coliform	BRK	0.36*	0.26*	0.56*	0.58*
	PCH	0.40*	0.58*	0.37*	0.55*
E. coli	BRK	0.33*	0.35*	0.04	0.39*
	PCH	0.28*	0.33*	0.10	0.22*
Enterococci	BRK	0.27*	0.47*	−0.02	0.36*
	PCH	0.23*	0.34*	0.04	0.24*

*Significant at the 0.01 level (2-tailed).

Table 3
Comparison between predicted and measured geometric mean bacteria concentrations [log10(MPN/100 ml)]

	Station	Bird source	Sed. source	Runoff source	Combined	Measured
Total coliform	BRK	−1.12 (+0.49/−0.43)	2.14 (+0.45/−1.02)	0.81 (+0.20/−0.47)	2.42 (+0.45/−1.02)	2.38 (±0.03)
	PCH	−1.39 (+0.49/−0.43)	2.25 (+0.45/−1.02)	−0.18 (+0.20/−0.47)	2.33 (+0.45/−1.02)	2.17 (±0.04)
E. coli	BRK	−1.38 (+0.83/−0.40)	0.76 (+0.63/−1.21)	−0.36 (+0.20/−0.44)	1.10 (+0.63/−1.21)	1.49 (±0.03)
	PCH	−1.65 (+0.83/−0.40)	0.86 (+0.63/−1.21)	−1.35 (+0.20/−0.44)	0.98 (+0.63/−1.21)	1.53 (±0.03)
Enterococci	BRK	−1.56 (+0.56/−0.44)	1.39 (+0.43/−0.98)	−0.11 (+0.18/−0.44)	1.61 (+0.43/−0.98)	1.34 (±0.03)
	PCH	−1.85 (+0.56/−0.44)	1.42 (+0.43/−0.98)	−1.10 (+0.18/−0.44)	1.49 (+0.43/−0.98)	1.38 (±0.04)

Uncertainty of predictions is shown along with standard error of measurements ($N = 360$).

Table 4
Pearson correlation between turbidity measurements and bacteria predictions and measurements for first six days of study ($N = 144$)

	Station	Sed. source	Runoff source	Combined	Measured
Total coliform	BRK	0.19	0.70*	0.51*	0.56*
	PCH	0.57*	0.47*	0.59*	0.41*
E. coli	BRK	0.20	0.70*	0.56*	0.20
	PCH	0.57*	0.48*	0.60*	0.14
Enterococci	BRK	0.26*	0.70*	0.53*	0.31*
	PCH	0.58*	0.47*	0.60*	0.14

*Significant at the 0.01 level (2-tailed).

dependent settling rates are also known. This would be particularly important if FIB were associated with particles larger than 10–15 μm, in which case accurate settling data would be crucial for reliable predictions.

Both turbidity and FIB are generally associated with fine particles, but in this as well as previous studies (Goyal et al., 1977; Jensen et al., 1979) a strong association between the two has not been observed. In Talbert Marsh, peaks in turbidity and TC are observed at low tide, when brackish water from the upper reaches of the wetland is translated furthest seaward (Figs. 4 and 5). Hence, urban runoff is clearly contributing to the TC signal. On the other hand, there are not clearly defined peaks in the EC and ENT measurements and in many cases EC and ENT are elevated when turbidity values are relatively small. If sediments are the source of these FIB, a possibility strongly supported by model predictions shown here, shear stresses on the bed must be large enough to disturb and saltate surficial sediments, large enough to mix small particles, colloidal matter, and FIB through the water column, but not large enough to suspend the sandy sediments more than a short distance above the bed. Recall that sediments consist of beach sands and silts near the outlet. Hence, water quality

models designed to account for the effects of sediment resuspension should be sensitive to differences between the rate of sediment entrainment, and the rate of FIB entrainment. Sediment entrainment formulations adopt the notion that mass transfer occurs when the shear stress on the bed exceeds a certain threshold (Mehta and Dyer, 1990). The entrainment of FIB in surficial pore water or incorporated into microbial biofilms may occur at a much smaller threshold.

The significance of loading due to sediment resuspension explains why tidal wetlands serve to "generate" FIB, as was reported by (Grant et al., 2001). That is, FIB associated with sediment particles, colloidal organic matter, or free living in porewater are supplied to the water column when bottom sediments are disturbed and/or scoured by tidal currents. FIB input to wetlands from wet or dry weather surface water runoff may be temporarily stored in sediments and later resuspended during storm events or during tidal scouring. The relative magnitude of resuspension effects versus die-off and settling effects is likely to control whether or not coastal wetlands are net generators or net accumulators. The results of this study are important to temper expectations that hydrodynamically-active wetlands such as estuaries or streams can provide passive treatment of urban runoff with high concentrations of FIB.

Reeves et al. (2004) reported that over 99% of the annual load of FIB from Talbert Watershed runoff is shed during storm events, while less than 1% is shed during dry-weather periods. It is therefore likely that sediments serve to couple FIB loads from storm water runoff to dry-weather water quality. Additional studies are warranted to characterize the variability of FIB in sediments over seasonal to tidal time scales and in response to storm events, to characterize the spatial variability of FIB, and to understand the mechanisms driving this variability. Do these organisms die-off, deposit, stimulate regrowth, and/or pass through the wetland? Microbiological source tracking methods (DNA fingerprinting, etc.) could also be applied to assess whether FIB in sediments are linked to human sources of fecal pollution (Simpson et al., 2002; Scott et al., 2002).

5. Conclusions

This study successfully employed a first-principle model to predict the dry-weather tidal cycling of FIB in Talbert Marsh, an estuarine, intertidal wetland in Huntington Beach, California. Model predictions show that surface water concentrations of TC, EC, and ENT in the wetland are driven by loads from urban runoff and resuspended wetland sediments. The model more accurately predicts TC than EC or ENT.

The crucial role that sediments play in the cycling of FIB is highlighted by this study. Sediments function as a reservoir of FIB that may accumulate FIB due to regrowth or settling, or shed FIB when tidal currents or storm flows scour away or even just disturb surficial particles. This finding is important to temper expectations that hydrodynamically-active wetlands serve to "treat" FIB from runoff and other sources, and it also explains why wetlands can function as net generators of surface water FIB. That is, generation occurs when the entrainment rate exceeds the rate of die-off and settling.

Additional studies should be conducted to characterized the "memory" of sediments relative to FIB. Knowing the extent to which dry-weather sediment concentrations of FIB are linked to wet-weather runoff loads, dry-weather runoff loads, regrowth or other factors such as bird droppings would help determine which factors predominatly control dry-weather water quality. Additional studies should also be conducted to evaluate the size and settling velocities of particles associated with FIB, and the partitioning of FIB between free-living and particle-associated states. Improved predictions of FIB might result from separately modeling free-living and particle-associated FIB.

References

Ahn, J.H., Grant, S.B., Surbeck, C.Q., DiGiacomo, P.M., Nezlin, N.P., Jiang, S., 2005. Coastal water quality impact of storm water runoff from an urban watershed in southern California. Environmental Science and Technology, in press.

Alderisio, K.A., DeLuca, N., 1999. Seasonal enumeration of fecal coliform bacteria from the feces of ring-billed gulls (*Larus delawarensis*) and Canada geese (*Branta canadensis*). Applied and Environmental Microbiology 65 (12), 5628–5630.

American Public Health Association (APHA). Standard Methods for the Analysis of Water and Wastewater, 18th ed.

Ambrose, R.F., 2004. Pers. comm.

Anderson, S.A., Turner, S.J., Lewis, G.D., 1997. Enterococci in the New Zealand environment: implications for water quality monitoring. Water Science and Technology 35 (11–12), 171–174.

Arega, F., Sanders, B.F., 2004. Dispersion model for tidal wetlands. Journal of Hydraulic Engineering 130 (8), 739–754.

Byappanahalli, M.N., Fujioka, R.S., 1998. Evidence that tropical soil environment can support the growth of *Escherichia coli*. Water Science and Technology 38 (12), 171–174.

California Environmental Protection Agency, (CalEPA) 2002. 2002 Revision of the Clean Water Act Section 303(d) List of Water Quality Limited Segments. California State Water Resources Control Board, California Environmental Protection Agency, Sacramento, CA. http://www.swrcb.ca.gov/tmdl/303d_lists.html

Chu, A.K., 2001. Quantifying pollutant loading to coastal waters from an urban estuarine waterway. MS Thesis in Civil Engineering, University of California, Irvine.

Davies, C., Long, J., Donald, M., Ashbolt, N., 1995. Survival of fecal microorganisms in marine and freshwater sediments. Applied and Environmental Microbiology 61, 1888–1896.

Decho, A.W., 2000. Microbial biofilms in intertidal systems: an overview. Continental Shelf Research 20 (10–11), 1257–1273.

Desmarais, T.R., Solo-Gabriele, H.M., Palmer, C.J., 2002. Influence of soil on fecal indicator organisms in a tidally influenced subtropical environment. Applied and Environmental Microbiology 68 (3), 1165–1172.

Elder, J.W., 1959. The dispersion of marked fluid in turbulent shear flow. Journal of Fluid Mechanics 5, 544–560.

Fiandrino, A., Martin, Y., Got, P., Bonnefont, J.L., Trousselier, M., 2003. Bacterial contamination of Mediterranean coastal seawater as affected by riverine inputs: simulation approach applied to a shellfish breeding area (Thau lagoon, France). Water Research 37, 1711–1722.

Fujioka, R., Sian-Denton, C., Borja, M., Castro, J., Morphew, K., 1999. Soil, the environmental source of *Escherichia coli* and enterococci in Guam's streams. Journal of Applied Microbiology 85, 83S–89S.

Gould, D.J., Fletcher, M.R., 1978. Gull droppings and their effects on water quality. Water Research 12, 665–672.

Goyal, S.M., Gerba, C.P., Melnick, J.L., 1977. Occurrence and distribution of bacterial indicators and pathogens in canal communities along the Texas coast. Applied and Environmental Microbiology 34, 139–149.

Grant, S.B., Sanders, B.F., Boehm, A.B., Redman, J.A., Kim, J.H., Mrse, R., Chu, A.K., Gouldin, M., McGee, C., Gardiner, N., Jones, B.H., Svejkovsky, J., Leipzig, V., Brown, A., 2001. Generation of enterococci bacteria in a coastal wetland and its impact on surf zone water quality. Environmental Science and Technology 35 (12), 2407–2416 (samples collected in this study and processed for Enterococcus were also processed for Total coliform and *E. coli* using methods described in (Reeves et al., 2004). The resulting data were used in this study for model parameterization and validation purposes).

Grant, S.B., Sanders, B.F., Boehm, A., Arega, F., Ensari, S., Mrse, R., Kang, H.Y., Reeves, R., Kim, J.H., Redman, J., Jiang, S., Chu, W., Choi, S., Clark, C., Litz, L., Sutula, M., Noblet, J., Sobsey, M., McGee, C., 2002. Coastal runoff impact study phase II: sources and dynamics of fecal indicators in the lower Santa Ana River watershed. Report prepared for the National Water Research Institute, County of Orange, and the Santa Ana Regional Water Quality Control Board.

Grimes, D.J., Atwell, R.W., Brayton, P.R., Palmer, L.M., Rollins, D.M., Roszak, D.B., Singleton, F.L., Tamplin, M.L., Colwell, R.R., 1986. The fate of enteric pathogenic bacteria in estuarine and marine environments. Microbiological Sciences 3 (11), 324–329.

Hardina, C.M., Fujioka, R.S., 1991. Soil—the environmental source of *escherichia-coli* and enterococci in Hawaii streams. Environmental Toxicology and Water Quality 6 (2), 185–195.

Holman, J.P., 1978. Experimental Methods for Engineers. McGraw Hill, New York 493.

Hussong, D., Damare, J.M., Limpert, R.J., Sladen, W.J.L., Weiner, R.M., Colwell, R.R., 1979. Microbial impact of canada geese (*Branta canadensis*) and whistling swans (*Cygnus columbianus columbianus*) on aquatic ecolsystems. Applied and Environmental Microbiology 37 (1), 14–20.

Jensen, P., Rola, R., Tyrawski, J., 1979. Tidal wetlands and estuarine coliform bacteria. In: Hamilton, P., Macdonald, K.B. (Eds.), Estuarine and Wetland Processes. Plenum Press, New York, pp. 385–399.

Kashefipour, S.M., Lin, B., Harris, E., Falconer, R.A., 2002. Hydro-environmental modelling for bathing water compliance of an estuarine basin. Water Research 36, 1854–1868.

LaBelle, R.L., Gerba, C.P., Goyal, S.M., Melnick, J.L., Cech, I., Bogdan, G.F., 1980. Relationships between environmental factors, bacterial indicators, and the occurrence of enteric viruses in estuarine sediments. Applied and Environmental Microbiology 39, 588–596.

Mehta, A.J., Dyer, K.R., 1990. Cohesive sediment transport in estuarine and coastal waters. In: Le Mehaute, B., Hanes, D.M. (Eds.), The Sea Ideas and Observations on Progress in the Study of the Seas, vol. 9. Ocean Engineering Science, Wiley, New York.

Nazaroff, W.W., Alvarez-Cohen, L., 2001. Environmental Engineering Science, 690.

Oshiro, R., Fujioka, R., 1995. Sand, soil, and pigeon droppings—sources of indicator bacteria in the waters of Hanauma Bay, Oahu, Hawaii. Water Science and Technology 31 (5–6), 251–254.

Partheniades, E., 1965. Erosion and deposition of cohesive sediments. Journal of the Hydraulics Division ASCE 91 (1), 105–139.

Reeves, R.L., Grant, S.B., Mrse, R.D., Copil-Oancea, C.M., Sanders, B.F., Boehm, A.B., 2004. Scaling and management of fecal indicator bacteria in runoff from a Coastal Urban Watershed in southern California. Environmental Science and Technology 38 (9), 2637–2648.

Roper, M.M., Marshall, K.C., 1979. Effects of salinity on sedimentation and of particulates on survival of bacteria in estuarine habitats. Geomicrobiology Journal 1 (2), 103–116.

Savage, W.G., 1905. Bacteriological examination of tidal mud as an index of pollution of the river. Journal of Hygiene 5, 146–174.

Scott, T.M., Rose, J.B., Jenkins, T.M., Farrah, S.R., Lukasik, J., et al., 2002. Microbial source tracking: Current methodology and future directions. Applied and Environmental Microbiology 68 (12), 5796–5803.

Simpson, J.M., Santo Domingo, J.W., Reasoner, D.J., 2002. Microbial source tracking: state of the science. Environmental Science and Technology 36 (24), 5279–5288.

Sinton, L.W., Finlay, R.K., Lynch, P.A., 1999. Sunlight inactivation of fecal bacteriophages and bacteria in sewage-polluted seawater. Applied and Environmental Microbiology 65 (8), 3605–3613.

Solo-Gabriele, H.M., Wolfert, M.A., Desmarais, T.R., Palmer, C.A., 2000. Sources of *Escherichia coli* in a coastal subtropical environment. Applied and Environmental Microbiology 66 (1), 230–237.

Steets, B.M., Holden, P.A., 2003. A mechanistic model of runoff-associated fecal coliform fate and transport through a coastal lagoon. Water Research 37, 589–608.

Tattersall, G.R., Elliot, A.J., Lynn, N.M., 2003. Suspended sediment concentrations in the Tamar estuary. Estuarine, Coastal and Shelf Science 57, 679–688.

Taylor, B.N., Kuyatt, C.E., 1994. Guidelines for evaluating and expressing the uncertainty of NIST measurement results. NIST Technical Note 1297. National Institute of Standards and Technology, Gaithersburg, Maryland.

Thomann, R.V., Mueller, J.A., 1987. Principles of Surface Water Quality Modeling and Control. Harper Collins.

Uncles, R.J., Stephens, J.A., 1989. Distributions of suspended sediment at high water in a macrotidal estuary. Journal of Geophysical Research 94, 14395–14405.

US Environmental Protection Agency (US EPA) (1986) Ambient water quality criteria for bacteria. EPA A440/5-84-002. US Environmental Protection Agency, Washington, DC.

Ward, P., 1974. Transverse dispersion in oscillatory channel flow. Journal of the Hydraulics Division 100 (HY6), 755–770.

Modeling the dry-weather tidal cycling of fecal indicator bacteria in surface waters of an intertidal wetland

Brett F. Sanders[a,*], Feleke Arega[a,1] and Martha Sutula[b]

[a]Department of Civil and Environmental Engineering, University of California, Irvine, CA 92697-2175, USA

[b]Southern California Coastal Water Research Project, Westminster, California, USA

Received 30 August 2004; revised 19 May 2005; accepted 2 June 2005. Available online 26 July 2005.

Abstract

Recreational water quality at beaches in California and elsewhere is often poor near the outlets of rivers, estuaries, and lagoons. This condition has prompted interest in the role of wetlands in modulating surface water concentrations of fecal indicator bacteria (FIB), the basis of water quality standards internationally. A model was developed and applied to predict the dry-weather tidal cycling of FIB in Talbert Marsh, an estuarine, intertidal wetland in Huntington Beach, California, in response to loads from urban runoff, bird feces, and resuspended sediments. The model predicts the advection, dispersion and die-off of total coliform, *Escherichia coli*, and enterococci using a depth-integrated formulation. We find that urban runoff and resuspension of contaminated wetland sediments are responsible for surface water concentrations of FIB in the wetland. Model predictions show that urban runoff controls surface water concentrations at inland sites and sediment resuspension controls surface water concentrations near the mouth. Direct wash-off of bird feces into the surface water is not a significant contributor, although bird feces can contribute to the sediment bacteria load. The key parameters needed to accurately predict FIB concentrations, using a validated hydrodynamic model, are: the load due to urban runoff, sediment erodibility parameters, and sediment concentrations and surface water die-off rates of enteric bacteria. In the present study, literature values for sediment erodibility and water column die-off rates are used and average concentrations of FIB are predicted within 1/2 log unit of measurements. Total coliform are predicted more accurately than *E. coli* or enterococci, both in terms of magnitude and tidal variability. Since wetland-dependent animals are natural sources of FIB, and FIB survive for long periods of time and may multiply in wetland sediments, these results highlight limitations of FIB as indicators of human fecal pollution in and near wetlands.